Princeton Plasma Physics Laboratory

PPPL-5326

Effects of Magnetic Islands on Bootstrap Current in Toroidal Plasmas

G. Dong, Z. Lin

December 2016

Prepared for the U.S. Department of Energy under Contract DE-AC02-09CH11466.

Princeton Plasma Physics Laboratory
Report Disclaimers

Full Legal Disclaimer

Trademark Disclaimer

PPPL Report Availability

Princeton Plasma Physics Laboratory:

http://www.pppl.gov/techreports.cfm

Office of Scientific and Technical Information (OSTI):

http://www.osti.gov/scitech/

Related Links:

U.S. Department of Energy

U.S. Department of Energy Office of Science

U.S. Department of Energy Office of Fusion Energy Sciences

Effects of Magnetic Islands on Bootstrap Current in Toroidal Plasmas

G. Dong[1], Z. Lin[2,(a)]

[1] Princeton Plasma Physics Laboratory, Princeton, NJ, 08540, USA

[2] Department of Physics and Astronomy, University of California, Irvine, CA 92697, USA

[(a)] Author to whom correspondence should be addressed.

E-mail: zhihongl@uci.edu

Aug 10th, 2016

Abstract

The effects of magnetic islands on electron bootstrap current in toroidal plasmas are studied using gyrokinetic simulations. The magnetic islands cause little changes of the bootstrap current level in the banana regime because of trapped electron effects. In the plateau regime, the bootstrap current is completely suppressed at the island centers due to the destruction of trapped electron orbits by collisions and the flattening of pressure profiles by the islands. In the collisional regime, small but finite bootstrap current can exist inside the islands because of the pressure gradients created by large collisional transport across the islands. Finally, simulation results show that the bootstrap current level increases near the island separatrix due to steeper local density gradients.

I. Introduction

Kinetic effects at microscopic scales play important roles in the evolution of macroscopic magnetohydrodynamic (MHD) modes such as neoclassical tearing modes (NTM) [1, 2], rendering global kinetic simulations of toroidal plasmas a necessity. The dominant features of NTMs are magnetic islands driven by helical perturbations of the bootstrap current [3] in the vicinity of mode rational surfaces. Large magnetic islands can degrade confinement properties and even lead to disruptions in fusion reactors [4]. Therefore, predictive capability needs to be established for NTM in next-step fusion devices such as ITER [5].

The NTM dynamics involve the coupling of neoclassical effects, microturbulence, and island dynamics, which largely differ from one another in their spatial and temporal scales [4, 6, 7]. Kinetic [8-11] and fluid [12-13] simulations addressing the coupling of multiple physical processes have been carried out in recent years for NTM studies. Resolving disparate spatiotemporal scales is necessary for the understanding of NTM physics, including the threshold of seed island size, island growth rate, and nonlinear dynamics. Numerical difficulties associated with kinetic simulations of the tearing modes make self-consistent NTM simulations even more arduous. The motivation of this work is thus to develop the kinetic NTM simulation capability including the interactions of magnetic islands, bootstrap current, microturbulence, and energetic particles.

Bootstrap current is a self-generated parallel current resulting from pressure gradients and collisional effects in the toroidal geometry [14], and can greatly enhance the plasma confinement. It is roughly proportional to the radial pressure gradients of trapped electrons in the toroidal plasmas [3]. The conventional wisdom is that magnetic islands can reduce the electron pressure gradients through rapid parallel transport, and consequentially reduce the bootstrap current. The reduction in the bootstrap current in turn causes a magnetic perturbation to amplify the islands. Therefore, an accurate calculation of the bootstrap current in response to the islands is important for understanding the NTM drive, especially the threshold of the seed islands.

W. A. Hornsby et al. [15] used a minimal drift-kinetic model to demonstrate the effects of magnetic islands and turbulent transport on the electron profiles and the bootstrap current, and showed that finite pressure gradients (and associated bootstrap current) can exist within the islands when turbulent transport is sufficiently strong. E. Poli et al. [16, 17] used Monte

Carlo simulations to study finite ion orbit width effects on the bootstrap current, and showed that a finite bootstrap current could exist within the islands when the island width is comparable to the ion orbit width. A. Bergmann et al. [18] found that when the islands are rotating at the electron diamagnetic frequency, bootstrap current could be completely preserved due to small island effects. The rotation of the islands also affects the pressure profile flattening [22].

In this work, we use Gyrokinetic Toroidal Code (GTC) [19] to study the effects of magnetic islands on neoclassical transport. P. Jiang et al. [20, 21] implemented magnetic islands in the GTC to study the effects of magnetic islands on drift wave instabilities, where neoclassical effects were not included. In the current simulations, the flattening of the pressure gradients by the islands is verified first. The electron neoclassical transport level is also verified in the simulations without the islands. The bootstrap current level from simulations without the islands agrees very well with analytical results.

In this paper, the effects of the static magnetic islands on the electron bootstrap current are studied for various collisionality regimes in the absence of microturbulence. Surprisingly, magnetic islands cause little changes of the bootstrap current level in the banana regime because of trapped electron effects. As the collision frequency increases to the plateau regime, the bootstrap current is completely suppressed at the island centers due to the destruction of trapped electron orbits by collisions and the flattening of pressure profiles by the islands. In the collisional regime, a small but finite bootstrap current can exist inside the islands because of the pressure gradients created by large collisional transport across the islands. Finally, simulation results show that the bootstrap current level increases near the island separatrix due to steeper local density gradients.

The reason that magnetic islands does not suppress the bootstrap current in the banana regime is that trapped electrons are mostly not affected by the islands. The remaining trapped electron pressure gradients create an anisotropy in the parallel velocity, which induces a parallel flow of the passing electrons by the collisional friction force across the trapped-passing boundary. Therefore, the bootstrap current can survive inside the islands even though the pressure profiles of the passing electrons are flattened by the islands. These simulation results could have significant implications to the theory of NTM excitation based on the conventional picture of islands suppressing the bootstrap current by flattening the pressure profiles. Our

simulations thus call for better understanding of the effects of magnetic islands on the bootstrap current using fully self-consistent simulations.

The rest of this paper is arranged as follows: formulation and verification of the simulation scheme is presented in Section II, followed by the simulation results of the island effects on the bootstrap current in Section III. In Section IV, we discuss the dependence of the bootstrap current on the collision frequency in the presence of the islands. In Section V, we summarize the main results and discuss future studies.

II. Formulation and verification of neoclassical simulations

1. Implementation of magnetic islands in GTC

First-principles gyrokinetic simulations of toroidal plasmas with magnetic islands superimposed on the equilibrium field are carried out using GTC, which has extensively been applied to study instabilities, turbulence, and transport in fusion plasmas [23-27]. In this work, GTC is utilized to study the effects of static magnetic islands on neoclassical bootstrap current.

In the simulations, we use magnetic coordinates (ψ, θ, ζ) representing, respectively, poloidal flux, poloidal, and toroidal angles. The equilibrium field is: $\mathbf{B}_0 = B_0\mathbf{b}_0 = q\nabla\psi\times\nabla\theta - \nabla\psi\times\nabla\zeta = \delta\nabla\psi + I\nabla\theta + g\nabla\zeta$, where q is the safety factor, g and I are the poloidal and toroidal currents (divided by 2π). The radial component δ arises from the non-orthogonality of the Boozer coordinates and is usually small for large aspect-ratio tokamaks [28]. The imposed static magnetic island perturbations are in the form of $\delta\mathbf{B} = \nabla\times\delta\mathbf{A}_{\parallel} = \nabla\times\alpha\mathbf{B}_0$, and $\alpha = \delta A_{\parallel}/B_0 = \alpha\cos(m\theta - n\zeta)$ is independent of the poloidal flux ψ for simplicity. Here m is the poloidal mode number and n is the toroidal mode number. If we consider $\nabla\times\mathbf{B}_0 = 0$ and neglect the δ -term, $\delta\mathbf{B}$ would be in the radial direction only. We can define the helical flux as $\psi_h = \psi - \psi_t/q_s - \alpha$ to represent the magnetic field geometry (solid line in Figure 3),where $q_s = m/n$, ψ_t is the toroidal flux function, so that $B\cdot\nabla\psi_h \cong 0$ [20]. Island separatrix is defined by $[\psi_h - (\psi - \psi_t/q_s)]^2 = 0$, giving the island half width (radial distance from O-point to the separatrix at $\theta = 0$) $w = R_0(\alpha_0 q_s/q_s')^{1/2}$, where $q_s' = dq/dr$ is the gradient of the q profile at the resonant surface.

2. Gyrokinetic simulation of neoclassical transport with magnetic islands

In GTC simulation, the dynamics of guiding centers are governed by the Hamiltonian in the phase space of $(\mathbf{X},\mu,v_{\|})$ [29],

$$H = \frac{1}{2}m_\alpha v_{\|}^2 + \mu B + q_\alpha \phi$$

where $\mathbf{X}$ denotes spatial coordinates, μ denotes magnetic moment and $v_{\|}$ denotes parallel velocity along the field line, m_α / q_α is the particle mass/charge for each species, B is magnetic field amplitude, and ϕ is gyrophase averaged electrostatic potential.

From canonical guiding center equations of motion [27], the gyrokinetic Vlasov equation with only neoclassical drive and static magnetic island is in the form of:

$$\frac{d}{dt}f = \frac{\partial f}{\partial t} + \dot{\mathbf{X}}\cdot\nabla f + \dot{v}_{\|}\frac{\partial f}{\partial v_{\|}} - \hat{C}(f) = 0$$

$$\dot{\mathbf{X}} = v_{\|}\frac{\mathbf{B}}{B_0} + \mathbf{v}_d$$

$$\dot{v}_{\|} = -\frac{1}{m_\alpha}\frac{\mathbf{B}^*}{B}\cdot\mu\nabla B_0$$

where $f(\boldsymbol{X},\mu,v_{\|})$ is guiding center distribution function, $\mathbf{B} = \mathbf{B}_0 + \delta\mathbf{B}$, $\mathbf{B}^* = \mathbf{B}_0^* + \delta\mathbf{B}$, $\mathbf{B}_0^* = \mathbf{B}_0 + \frac{B_0 v_{\|}}{\Omega}\nabla\times\mathbf{b}_0$, and $\delta\mathbf{B}$ is the imposed island perturbation described in the last subsection.

The magnetic drift velocity is the sum of magnetic curvature and gradient drifts (neglecting island contributions to magnetic field magnitude):

$$\mathbf{v}_d = \frac{v_{\|}^2\nabla\times\mathbf{b}_0}{\Omega_\alpha} + \frac{\mu\mathbf{b}_0\times\nabla B_0}{m_\alpha\Omega_\alpha}$$

The Fokker-Planck collision operators $\hat{C}(f)$ include inter-species and like-species collisions that conserve particle number, momentum, and energy as described in Ref. [30].

A perturbative δf method is adopted for GTC neoclassical simulations [29, 31] to reduce particle noise with smaller number of particles and simpler particle loading profile compared with the full-f method. Here, particle distribution is separated into equilibrium and perturbed parts: $f = f_0 + \delta f$. The equilibrium distribution function f_0 satisfies

$$\frac{\partial f_0}{\partial t} + (v_{\parallel}\frac{\mathbf{B}_0}{B_0})\cdot\nabla f_0 + (-\frac{1}{m_\alpha}\frac{\mathbf{B}_0}{B_0}\cdot\mu\nabla B_0)\frac{\partial f_0}{\partial v_{\parallel}} - \hat{C}f_0 = 0.$$

The local Maxwellian equilibrium distribution function is an exact solution to the above equation in ($\mathbf{X}$, μ, $v_{\parallel}$) coordinates:

$$f_0 = \frac{n_0}{(2\pi T_0/m)^{3/2}}\exp[-\frac{2\mu B_0 + mv_{\parallel}^2}{2T_0}] .$$

We define a particle weight $w = \delta f / f$ and a gradient operator $\boldsymbol{\kappa} = \nabla n_0 / n_0 + (E/T_0 - 3/2)\nabla T_0 / T_0$. The weight equation can be derived from the perturbed distribution function and is expressed as:

$$\frac{dw}{dt} = (1-w)[-(v_{\parallel}\frac{\delta\mathbf{B}}{B_0} + \mathbf{v}_d)\cdot\boldsymbol{\kappa}]$$

The first term in the R.H.S. bracket is the magnetic flutter drive due to the guiding center parallel motion, and the second term is the neoclassical drive due to the perpendicular guiding center drifts. This weight equation and the guiding center orbit equations form a closed system of equations for gyrokinetic simulations of neoclassical transport in toroidal plasmas in the presence of magnetic islands.

3. Verification of GTC simulation of bootstrap current

In the simulations, uniform Maxwellian of electrons and ions are loaded over an annulus section of torus. We use representative plasma parameters with a major radius $R_0 = 1.86m$, a minor radius $a = 0.246R_0 = 86\rho_i$ (ρ_i is the ion gyroradius), a parabolic q profile $q = 1.475 + 1.1\frac{\psi}{\psi_w} + 1.0\frac{\psi^2}{\psi_w^2}$, a circular cross section and a hyperbolic density profile

$n_e = n_0[1.0 + 0.205(\tanh(0.3 - 2.5\frac{\psi}{\psi_w}) - 1.0)]$, with the poloidal flux function $\psi(r = a) = \psi_w$. At $r = 0.5a$, Z_{eff}=1.5, $B_0 = 1.35T$, $T_i = T_e = 5.0keV$, $q = 2.0$, $R_0/L_n = 2.2$ (L_n is the density gradient scale length). The effective collision frequency is defined as the physical collision frequency normalized by the bounce frequency $\nu^* = \varepsilon^{-3/2}\nu qR_0 / v_{th}$, where $\varepsilon = r / R_0$ is the local inverse aspect ratio, $v_{th} = (T / m)^{1/2}$ is the particle thermal velocity. With these parameters, $\nu^* = 0.028$, corresponding to the core of present day tokamak plasmas. A total of 1.25×10^7 particles are used in the simulations. The electron particle flux is $\Gamma = \int v_d \delta f_e d\mathbf{v}$, energy flux is $Q = \int v_d mv^2 / 2 \delta f_e d\mathbf{v}$, and bootstrap current density is $j_b = \int v_{\parallel} \delta f_e / (1 + \varepsilon \cos\theta) d\mathbf{v}$. Flux-surface averaging is applied to all neoclassical fluxes [29].

Collision frequency is scanned and details of the neoclassical transport are first investigated in the absence of the islands to verify the numerical scheme in the neoclassical simulations. The calculated neoclassical flux values agree well with the analytic expressions for the large aspect ratio tokamak in Ref. [3]. The bootstrap current j_b in the absence of magnetic islands from the simulations with different collision frequencies are presented as blue crosses in Figure 1. For comparisons, results from the analytic expression [3] is also plotted as the black line in Figure 1. The bootstrap current is normalized by the value at small collision frequency limit $j_0 = 1.46 \cdot \sqrt{\varepsilon} \frac{c}{B_{p0}} \frac{dP}{dr}$. GTC results agree quite well with the analytical results in the banana, plateau, and collisional regimes, with an average error of 3.3%.

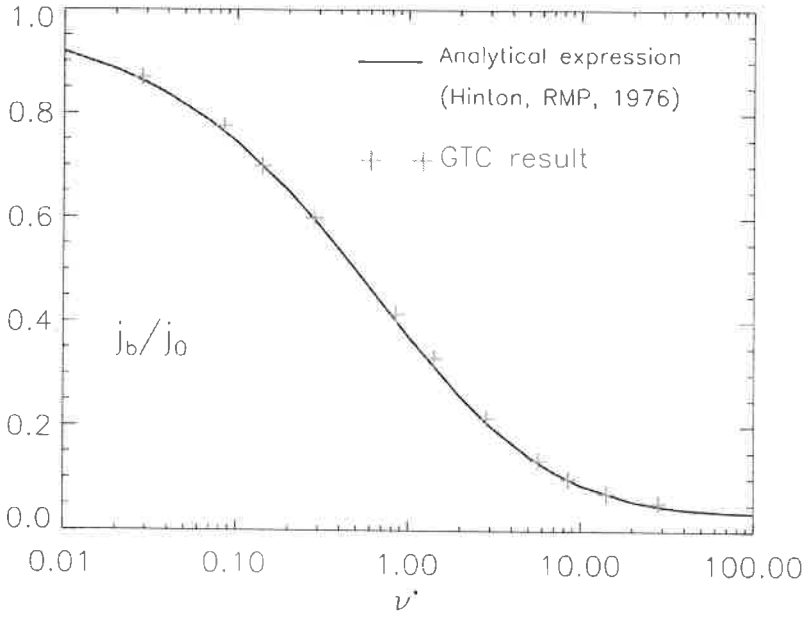

FIGURE 1: Bootstrap current j_b dependence on collision frequency ν^* without magnetic islands. The solid line is the analytic expression in Ref [3].

4. Verification of density flattening by magnetic islands

The m=2, n=1 islands, which are most catastrophic for some tokamak experiments, are now added to the equilibrium magnetic field. The islands are static and non-rotating, and center at r = 0.5a with an island width of w=12ρ_i. Due to the fast parallel transport, the electron and ion density profiles flatten inside the island area. At the low field side $\theta = 0$, where the toroidally trapped particles are present, the flattening of the density profile is smaller than that at the high field side $\theta = \pi$, where there are no trapped particles. To verify the validity of the island formulation, the electron and ion density profile changes by the islands are investigated in detail. The density flattening is illustrated in Figure 2, where collisionless plasmas are considered so that the particle orbits are Hamiltonian (stochasticity may still exist in small region near the island separatrices due to numerical dissipations). The electron and ion density profiles are measured locally in $\theta = 0$ or $\theta = \pi$ (averaged over $\Delta\theta = 0.005\pi$), and $\zeta = 0$ (averaged over $\Delta\zeta = 0.03\pi$), and averaged over one bounce time after the density profiles and the neoclassical fluxes reach the steady state. At the center of the simulation domain $r = 43\rho_i, \varepsilon = 0.12$, $q = 2.0$.

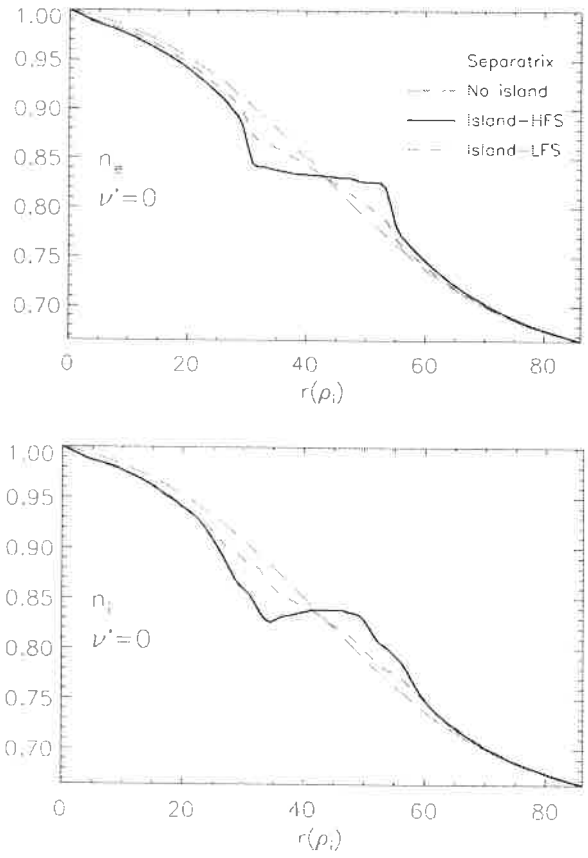

FIGURE 2: Electron (upper panel) and ion (lower panel) density profiles in collisionless plasmas. The black solid lines are density profiles at the high field side. The red-dashed lines are density profiles at the low field side. The two vertical lines represent the island separatrices. The blue-dashed lines are the density profiles without magnetic islands.

The initial radial density profiles are hyperbolic, as indicated by the blue dashed lines, which change little in the absence of islands. However, in the presence of the islands, the density profiles flatten inside the island and reach the steady state in a few bounce times. When the collision frequency is small, the toroidally trapped particles (mostly at the low field side) do not follow the entire field lines around the islands. Therefore, the trapped particles at the low field side retain their initial radial density profiles, resulting in a less flattened density profile at the low field side in the banana regime.

From Figure 2, the ion density profile at the low field side only has a small deviation from the equilibrium profile. The electron density profile has ~ 40 % flattening, which is close to the passing fraction $1-f_t = 1-1.46\varepsilon^{1/2} \sim 0.49$. This result is consistent with that of W. A. Hornsby et al in Ref. [8]. The fact that the ion density profile at the low field side is less flattened might be

caused by the finite passing orbit width $\sim q\rho_i$. The passing ion orbit width is not negligible compared with the island size, while the passing electron orbit width is negligible. This picture is confirmed by the electron and ion poloidal density perturbation contour plots shown in Figure 3, in which the electron density perturbation shows a clearer island shape while the ion density perturbation is blurrier.

Figure 2 shows that at the high field side, ion density profile is almost completely flattened in the island center, while the electron density profile maintains a finite gradient. This difference might be caused by island trapping of the electrons. The island trapping term is included in the simulations through the mirror force of the equilibrium magnetic field when the electrons move along the field line. Therefore, the islands will have their own "island-trapped electrons" with a trapped fraction proportional to the square-root of the island effective inverse aspect ratio $\varepsilon_{is} = w / R_0$. This effect causes the electrons to be trapped on the island "low field side", which is closer to the magnetic axis at the high field side ($\theta=\pi$). Ions will not have this effect since their island-trapped orbit width would be even larger than the island size, making them stay untrapped. The difference between ion and electron local density profiles might induce a parallel electric field inside the islands, which can in turn modify their profiles in fully self-consistent simulations. This self-consistent ambipolar field can be an important physics in NTM dynamics that has not been addressed in conventional NTM theory.

With collisions, the electron and ion density profiles still flatten inside the islands, though the profile shape varies with the collision frequency. The collision frequency dependence of the electron density profiles is illustrated in Figure 6 and will be discussed in the later section.

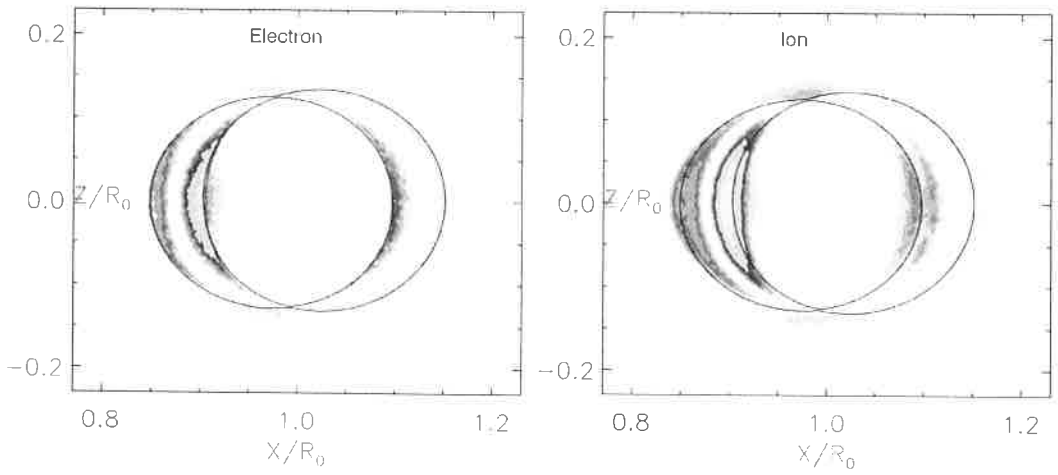

FIGURE 3: Poloidal contour plots of electron (upper panel) and ion (lower panel) perturbed density in collisionless plasmas with islands. The solid black lines are island separatrices. Red is positive density change and green is negative density change.

III. Effects of Magnetic Islands on Bootstrap Current

We now study the effects of magnetic islands on electron bootstrap current using island perturbations and plasma parameters described in Section II. For simplicity, only electrons are loaded in the simulations. Self-consistent electric field is not solved, and thus quasi-neutrality does not play any role in the present simulations. Electron particle flux and bootstrap current are measured in the simulations. As shown in Figure 4, the bootstrap current reaches the steady state in a few collision times in the plateau regime. The volume-integrated bootstrap current is not changed by the islands, although the radial profile changed drastically in the vicinity of the islands as shown in Figure 5.

The island induced radial particle transport, which slowly reaches the steady state after about ten collision times, is much larger than the neoclassical transport level calculated in the absence of the islands as shown in the lower panel of Figure 4. The electron density profile also reaches the steady state inside the islands on the same time scale. When the collision frequency is smaller, the electron particle flux drops closer to the neoclassical level calculated without the islands as shown in Figure 7. As the collision frequency increases, the magnetic islands induce a larger particle transport compared to the neoclassical level calculated without the islands. If ions are also simulated, the difference in the particle fluxes between ions and

electrons can induce an ambipolar radial electric field, which will eventually constrain the ion and electron particle fluxes to the same level.

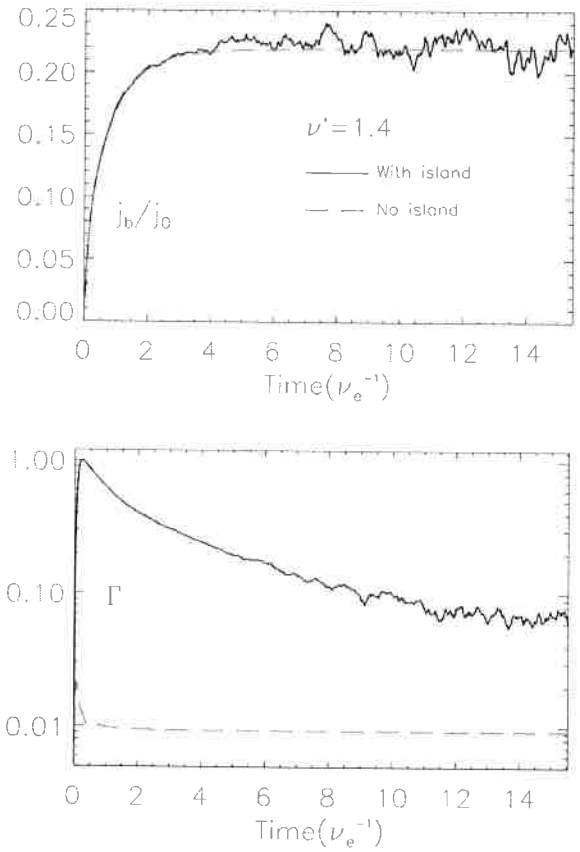

FIGURE 4: Time history of volume-integrated bootstrap current j_b (upper panel) and electron particle flux Γ (lower panel) in the plateau regime with (black-solid) and without (red-dashed) magnetic islands.

The bootstrap current and density profiles in the plateau regime ($\nu^*=1.4$) is illustrated in Figure 5. As the islands cause density flattening, the bootstrap current decreases dramatically inside the islands. On the other hand, the steepening of the density gradients outside the islands leads to a larger bootstrap current in the vicinity of the separatrix. If the bootstrap current accounts for a large fraction of the total plasma current, the variations in radial bootstrap current profiles can affect the q profile and local magnetic shear, and thus magnetohydrodynamic (MHD) stability properties. Outside the separatrices, the bootstrap current level has small radial oscillations, which correspond to the oscillations in the density gradient profiles. This can

be caused by the transport process: a steeper gradient causes a larger radial transport, resulting in a smaller gradient in the adjacent region, which would then steepen the gradient in the next adjacent region. This process seems to be analogous to the phase space oscillations in the standard Landau damping picture.

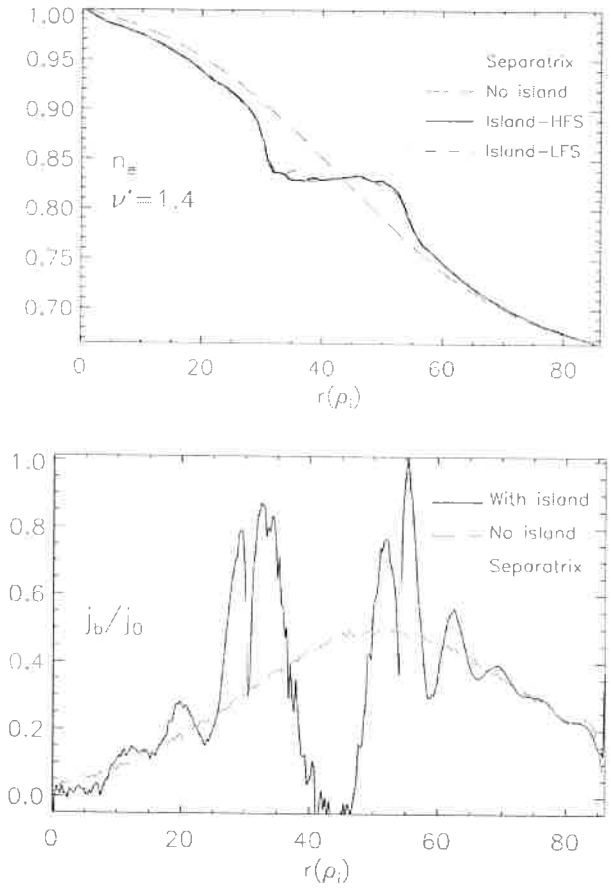

FIGURE 5: Radial profiles of bootstrap current (lower panel) and electron density (upper panel) in the plateau regime. The current and density profiles are averaged over one transit time. The two vertical lines represent the island separatrix.

IV. Collision Frequency Dependence of Bootstrap Current

The collision frequency is now scanned in the simulations with the islands to study the collision frequency dependence of bootstrap current. In the banana regime ($\nu^* < 1$), the trapped electron orbits are not fully destroyed by the collisions. They contribute to the finite density gradients inside the islands at the low field side, as illustrated by the red short-dashed lines in Figure 6. In the plateau regime ($\nu^* \sim 1$) where the collision time is comparable to the

trapped particle bounce time, the trapped particle orbits are mostly destroyed by collisions. Consequently, the trapped electron density profiles are gradually flattened inside the islands. The electron density profiles are now fully flattened at both high field and low field sides. Slightly reversed density profiles in the plateau regime are observed after a few collision times. The cause for this long time scale behavior will be investigated in the future work.

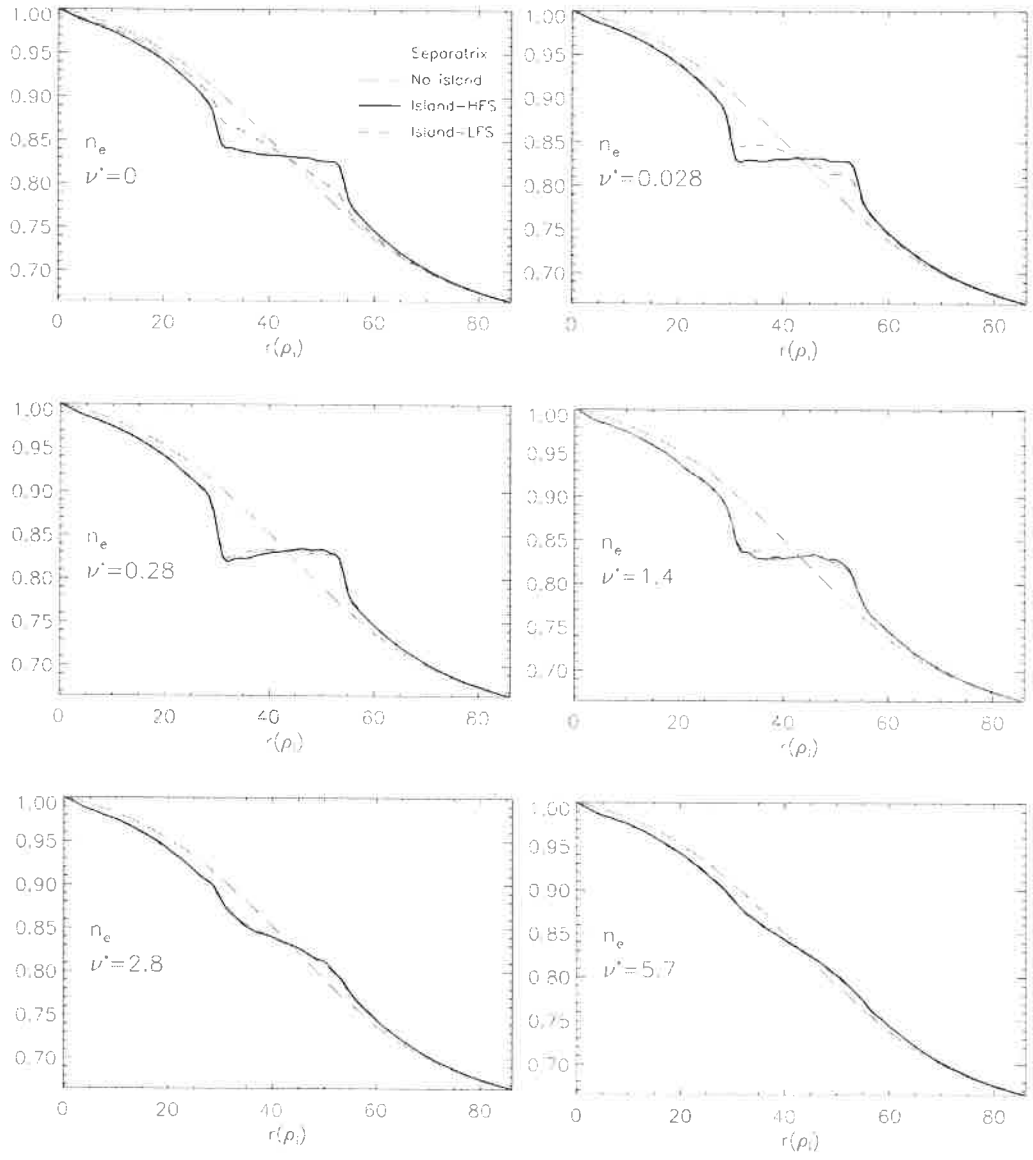

FIGURE 6: Collision frequency dependence of electron density profiles in the presence of islands. The black lines are the density profiles at the high field side. The red-dashed lines are the density profiles at the low field side. The vertical lines represent the separatrices. The blue-dashed lines are the electron density distributions without magnetic islands.

As the collision frequency increases further to the collisional regime ($\nu^* > 1$), the perpendicular transport becomes stronger. The balance between the perpendicular and parallel transport then leads to a finite density gradient in the island center [32]. The electron density gradients now increase with the collisionality at both the high field and low field sides, as shown in Figure 6. This mechanism is further illustrated by the collision frequency dependence of the electron particle fluxes in Figure 7. As the collision frequency increases, the magnetic islands induce a steady radial transport much larger than the neoclassical level in the absence of the islands.

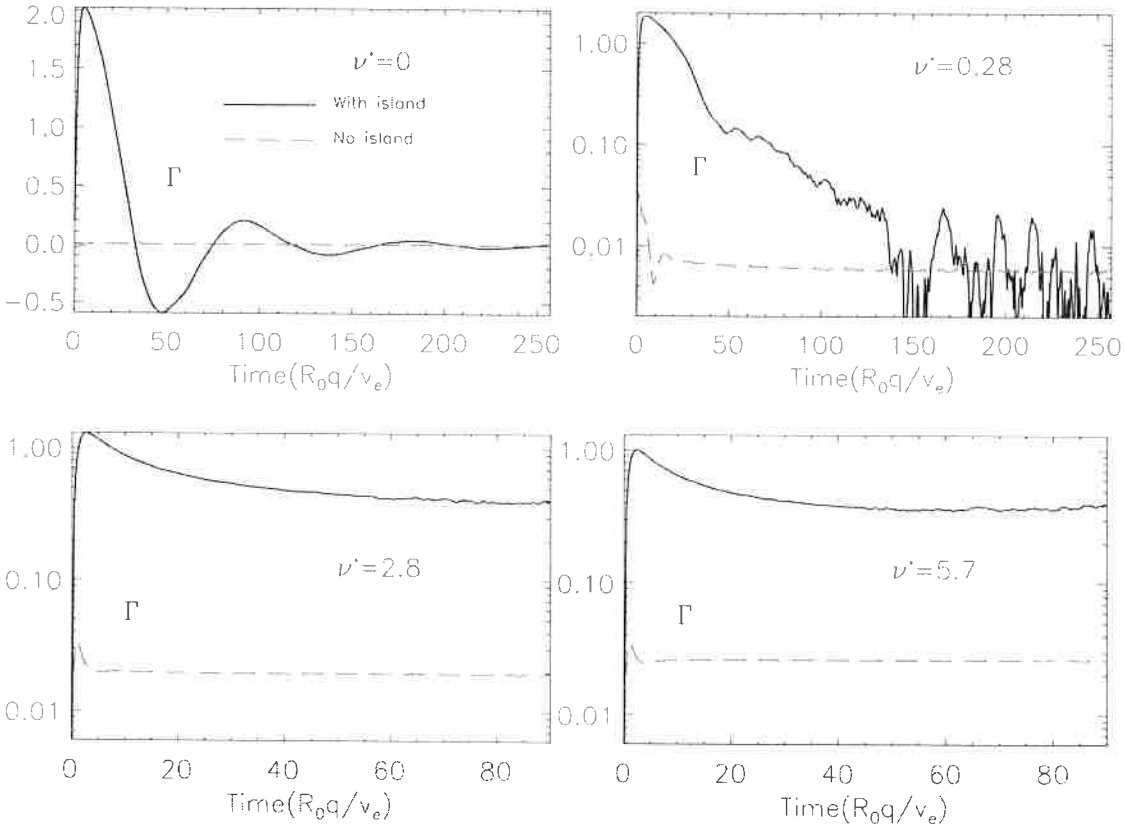

FIGURE 7: Time history of electron particle fluxes for various collision frequencies. The red-dashed lines are electron particle fluxes without magnetic islands. The black-solid lines are particle fluxes with magnetic islands.

In the banana regime, the bootstrap current level is almost unchanged by the magnetic islands as shown in Figure 8. The radial profiles of the bootstrap current are averaged over the unperturbed flux surface and over 40 times slices with a duration of about 3 R_0/c_s in simulation time. The trapped

particle orbits are mostly unperturbed by the collision, and therefore they do not follow the whole field lines around the islands. This effect results in a finite density gradient of the trapped particles, and therefore a finite bootstrap current level inside the islands even though the passing electron density profile is flattened. In the plateau and collisional regimes, the trapped electron orbits are mostly destroyed by collisions. The trapped electron density gradient reduction then leads to a sharp decrease of the bootstrap current inside the magnetic island. At the same time, the steepening of local pressure gradients outside the islands induces a larger bootstrap current at the vicinity of the islands. At a very high collisionality, the bootstrap current diminishes even though the large radial transport maintains strong density gradients inside the islands.

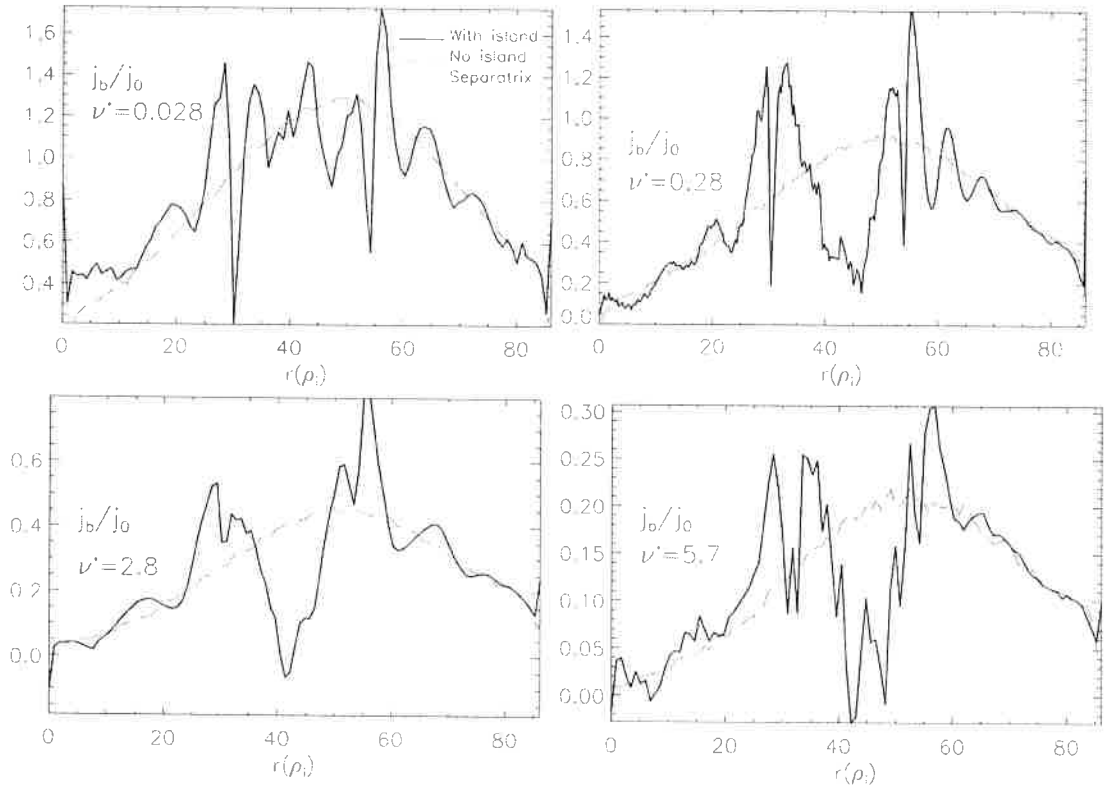

FIGURE 8: Radial profiles of bootstrap current for various collision frequencies. The blue-dashed lines are the bootstrap current profiles without the islands. The black-solid lines are the bootstrap current profiles with the islands. The vertical lines represent the separatrices.

The dependence of the island center bootstrap current j_{bis} on the collision frequency is shown in Figure 9, where the bootstrap current in the island center is averaged over $5\rho_i$ in the radial direction, and normalized by the

bootstrap current j_b at the same radial location in the simulations without magnetic islands. We can see that the bootstrap current at the island center is unaffected by the islands in the banana regime and fully suppressed by the islands in the plateau regime. There are small but finite bootstrap current in the collisional regime.

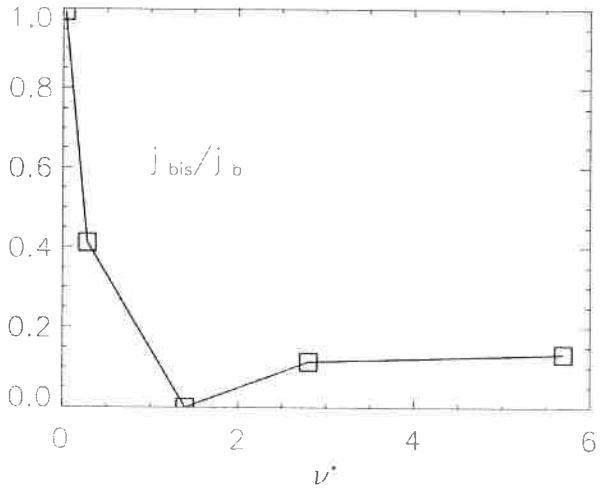

Figure 9: Collision frequency dependence of island center bootstrap current j_{bis}.

V. Conclusions

In this work we demonstrate that the electron bootstrap current suppression by the magnetic islands can be sensitive to the collision frequency in the toroidal plasmas. Drift kinetic electron simulation results show that in the banana regime, finite electron density gradients could exist in the islands at the low field side due to toroidally trapped electrons, and the bootstrap current level is only slightly perturbed by the magnetic islands. In the plateau regime, electron density profiles are flattened at both the high field side and the low field side, and the bootstrap current is completely suppressed at the island center. In the collisional regime, a small but finite bootstrap current can exist inside the islands because of the pressure gradients created by the large collisional transport across the islands. Near the separatrices, the island-induced transport results in steeper local density gradients, which lead to a larger local bootstrap current.

Electron temperature gradients also contribute to the bootstrap current. The temperature flattening by the islands [33] will thus affects the bootstrap current profile through the same physics as the density flattening. Therefore,

similar bootstrap current response to the islands can be expected. The ion contribution to the bootstrap current, which is not studied in the present work, could be subjected to the same physics. These results highlight the importance of including accurate trapped electron effects when studying the neoclassical tearing mode (NTM) dynamics. The conventional NTM theory using the reduced bootstrap current model probably predicts a larger effect of the islands on the bootstrap current, and thus a lower threshold of the seed island width. Our results also indicate that trapped electron modes can be less affected by the islands because of the trapped electron effects.

In the future work, we will focus on the first-principle simulations with magnetic islands, neoclassical transport, and self-consistent electric fields. The island rotation can have significant effects on the pressure flattening and the tearing mode dynamic when coupled with microturbulence. Therefore, incorporating the island rotation together with self-consistent electric fields is an important next step work. Microturbulence plays an important role as the transport mechanism [34], and could affect the bootstrap current level inside the islands. On the other hand, the islands could also suppress the turbulence and modify the turbulence spectrum. We would then be able to study the NTM physics with coupled dynamics of magnetic islands, microturbulence, neoclassical transport, and energetic particle effects [35].

Acknowledgments

The authors acknowledge useful discussions with J. Peng and GTC team. This work was supported by US Department of Energy (DOE) SciDAC GSEP Center (Grant No. DE-FC02-08ER54976) and China Scholarship Council (Grant No. 201206010268). Research at the Princeton Plasma Physics Laboratory is supported by the US DOE contract DE-AC02-09CH11466. This work used resources of the Oak Ridge Leadership Computing Facility at Oak Ridge National Laboratory (DOE Contract No. DE-AC05-00OR22725) and the National Energy Research Scientific Computing Center (DOE Contract No. DE-AC02-05CH11231).

Reference

[1] Z.Chang et al., Phys. Rev. Lett. 74, 4663 (1995)

[2] T. Oikawa et al., Phys. Rev. Lett. 94, 125003 (2005)

[3] F. L. Hinton and R. D. Hazeltine, Rev. Mod. Phys. 48, 239 (1976)

[4] R. J. La Haye, Phys. Plasmas 13, 055501 (2006)

[5] T. C. Hender et al., Nucl. Fusion 47, S128 (2007)

[6] E. Poli et al., Nucl. Fusion 49, 075010 (2009)

[7] L. Bardóczi et al., Phys. Rev. Lett. 116, 215001 (2016)

[8] W. A. Hornsby et al, Phys. Plasmas 17, 092301 (2010)

[9] R. E. Waltz and F. L. Waelbroeck, Phys. Plasmas 19, 032508 (2012)

[10] W. A. Hornsby et al., Plasma Phys. Control. Fusion 58, 014028 (2016)

[11] D. Zarzoso et al., Phys. Plasmas 22, 022127 (2015)

[12] O. Izacard et al, Phys. Plasmas 23, 022304 (2016)

[13] A. Ishizawa and F. L. Waelbroeck, Phys. Plasmas 20, 122301 (2013)

[14] R. J. Bickerton, J. W. Connor and J. B. Taylor 229, 110 (1971)

[15] W. A. Hornsby, et al., Plasma Phys. Control. Fusion 53, 054008 (2011)

[16] E. Poli, et al., Plasma Phys. Control. Fusion 45, 71-87 (2003)

[17] E. Poli, et al., Plasma Physics Reports, 42, 450–464 (2016)

[18] A. Bergmann, E. Poli, and A. G. Peeters, Phys. Plasmas, 16, 092507 (2009)

[19] Z. Lin, et al., Science, 281, 1835 (1998)

[20] P. Jiang, et al. Physics. Plasmas, 21, 122513 (2014)

[21] P. Jiang, el al. Plasma Science and Technology, 18, 126 (2016)

[22] D. Zarzoso et al., Nucl. Fusion 55, 113018 (2015)

[23] I. Holod, W. L. Zhang, Y. Xiao, and Z. Lin, Phys. Plasmas 16, 122307 (2009)

[24] Wenlu Zhang, Zhihong Lin, and Liu Chen, Phys. Rev. Lett. 101, 095001 (2008)

[25] Yong Xiao and Zhihong Lin, Phys. Rev. Lett. 103, 085004 (2009)

[26] H. S. Zhang, Z. Lin, and I. Holod, Phys. Rev. Lett. 109, 025001 (2012).

[27] Zhixuan Wang, et al., Phys. Rev. Lett. 111, 145003 (2013).

[28] R. B. White, The theory of toroidally confined plasmas, (2001)

[29] John R. Cary and Alain J. Brizard, Review of Modern Physics, 81, 693 (2009)

[30] Z. Lin, W. M. Tang, and W. W. Lee, Phys. Plasmas, 2 (8), 2975 (1995)

[31] Z. Lin, W. M. Tang, and W. W. Lee, Phys. Rev Lett., 78, 456 (1997)

[32] R. Fitzpatrick, Phys. Plasmas 2, 825 (1995)

[33] M. J. Choi, et al., Nucl. Fusion, 54, 083010 (2014)

[34] P. Hill, F. Hariri, and M. Ottaviani, Phys. Plasmas, 22, 042308 (2015)

[35] H. Cai, S. Wang, Y. Xu, J. Cao, and D. Li, Phys. Rev. Lett. 106, 075002 (2011)

PPPL PRINCETON PLASMA PHYSICS LABORATORY

Princeton Plasma Physics Laboratory
Office of Reports and Publications

Managed by
Princeton University

under contract with the
U.S. Department of Energy
(DE-AC02-09CH11466)

P.O. Box 451, Princeton, NJ 08543
Phone: 609-243-2245
Fax: 609-243-2751

E-mail: publications@pppl.gov

Website: http://www.pppl.gov